

Reductive and Oxidative Half-Reactions of Glutathione Reductase from *Escherichia coli*[†]

Patrick Rietveld,[‡] L. David Arscott,[§] Alan Berry,[‡] Nigel S. Scrutton,[‡] Mahendra P. Deonarain,[‡] Richard N. Perham,[‡] and Charles H. Williams, Jr.^{*,‡,§}

Department of Veterans Affairs Medical Center, Department of Biological Chemistry, University of Michigan, Ann Arbor, Michigan 48105, and Cambridge Centre for Molecular Recognition, Department of Biochemistry, University of Cambridge, Cambridge CB2 1QW, U.K.

Received April 11, 1994; Revised Manuscript Received August 17, 1994[®]

ABSTRACT: Glutathione reductase catalyzes the reduction of glutathione disulfide by NADPH and has a redox active disulfide and an FAD cofactor in each monomer. In the reductive half-reaction, FAD is reduced by NADPH and electrons pass from the reduced flavin to the redox active disulfide. The oxidative half-reaction is dithiol–disulfide interchange between the enzyme dithiol and glutathione disulfide. We have investigated the reductive and oxidative half-reactions using wild-type glutathione reductase from *Escherichia coli* and in an altered form of the enzyme in which the active site acid–base catalyst, His⁴³⁹, has been changed to an alanine residue (H439A). H439A has 0.3% activity in the NADPH/GSSG assay. The replacement affects both the oxidative half-reaction, as expected, and the reductive half-reaction—specifically, the passage of electrons from reduced flavin to the disulfide. Reduction of H439A by NADPH allows direct observation of flavin reduction. The NADPH–FAD charge transfer complex is formed in the dead time. Reduction of FAD, at a limiting rate of 250 s^{−1}, is observed as a decrease at 460 nm and an increase at 670 nm (FADH[−]–NADP⁺ charge transfer). Subsequent passage of electrons from FADH[−] to the disulfide (increase at 460 nm and a decrease at 670 nm) is very slow (6–7 s^{−1}) and concentration independent in H439A. The monophasic oxidative half-reaction is very slow, as expected for reduced H439A. The limiting rate of the reductive half-reaction in wild-type enzyme is independent of the NADPH concentration and determined to be 110 s^{−1}, while the limiting rate of the oxidative half-reaction has been estimated as 490 s^{−1}, and is dependent on the glutathione disulfide concentration. Thus, the acid–base catalyst participates in the disulfide reduction step by stabilizing the nascent thiolate and in the oxidative half-reaction by protonating the dissociating glutathione thiolate anion. Both roles are consistent with proposed mechanisms.

Glutathione reductase catalyzes the reduction of glutathione disulfide by NADPH. It is a member of the pyridine nucleotide disulfide oxidoreductase family of homodimeric flavoenzymes, having a redox active disulfide and an FAD cofactor in each monomer (Williams, 1992). The steps in the reductive half-reaction are shown in Scheme 1, where species II is an NADPH–FAD charge transfer complex; species III is an FADH[−]–NADP⁺ charge transfer complex; NADP⁺ is replaced by NADPH to give species IV and V; and reduction of the disulfide gives species VI, the thiolate–FAD charge transfer complex. NADPH enhances the thiolate–flavin charge transfer while NADP⁺ lowers the transition energy, shifting the band to longer wavelengths

(Williams et al., 1976). These spectral observations are a consequence of the fact that the pyridinium ring of NADPH or NADP⁺ and the isoalloxazine ring of FAD are parallel to one another as shown in Figure 7 (Karplus & Schulz, 1987) and thus interact electronically. FAD and NADP⁺ may act as a single acceptor in the charge transfer interaction in which the nascent thiolate is the donor. NADPH and thiolate are both donors to the FAD in species VI.

The reductive half-reaction was investigated by Huber and Brandt (1980) using the yeast enzyme at pH 7.6 and 5 °C. They observed three steps spectrally: the first, complete in the dead time of the apparatus (5 ms), was attributed to the formation of an NADPH–FAD charge-transfer complex. The second step, detected as an increase at 420 nm, had a limiting rate constant of 153 s^{−1} showing saturation kinetics ($K_D = 8.3 \mu\text{M}$). This step displayed a kinetic isotope effect of 2.7 with (4*S*)-[²H]NADPH which indicated that C–H bond breakage in NADPH takes place at this step. However, the increase at 420 nm and the lack of change at 460 nm would not be the expected spectral changes in flavin reduction. The third kinetically detectable step, forming the 540 nm absorbance characteristic of the thiolate–flavin charge transfer complex of 2-electron reduced enzyme, species VI, had a rate constant of 68 s^{−1} and was thus rate limiting in the overall half-reaction. NADP⁺ dissociation and NADPH binding precede or are concomitant with this step (Huber &

[†] This work has been supported by the Health Services and Research Administration of the Department of Veterans Affairs, by Grant GM-21444 from the National Institute of General Medical Sciences (C.H.W.), and by a grant from the Science and Engineering Research Council (R.N.P.). A.B. is a Royal Society 1983 University Research Fellow. M.P.D. was supported by a Research Studentship from the SERC and by a Benfactors' Research Scholarship from St. John's College. N.S.S. is a Research Fellow of the Royal Commission for the Exhibition of 1851 and a Research Fellow of St. John's College.

^{*} To whom correspondence should be addressed.

[‡] University of Michigan.

[§] Department of Veterans Affairs Medical Center.

[‡] University of Cambridge.

[®] Abstract published in *Advance ACS Abstracts*, October 15, 1994.

The diagram illustrates the proposed mechanism for the formation of a covalent intermediate in the FAD-dependent reaction of a protein. The scheme involves six states (I-VI) and three main steps.

State I: The initial state showing the protein (Cys42-S-Cys47-S-His439) and FAD. His439 is positioned to act as a general base for the reduction of FAD.

Step 1 (I to II): A fast equilibrium reaction where FAD is reduced to FADH⁻ by NADPH. The reaction is labeled "fast".

State II: The reduced state where FADH⁻ is formed, and His439 is now a thiolate (S⁻).

Step 2 (II to III): An equilibrium reaction with a rate constant of 310 s⁻¹. FADH⁻ is protonated at the N5 position of the isoalloxazine ring, forming a radical cation (H-N⁺).

State III: The radical cation state where the N5-H bond is formed.

Step 3 (III to IV): An equilibrium reaction with a rate constant of 250 s⁻¹. The N5-H bond is cleaved, forming a covalent intermediate (IV) with a disulfide bond between Cys42 and Cys47.

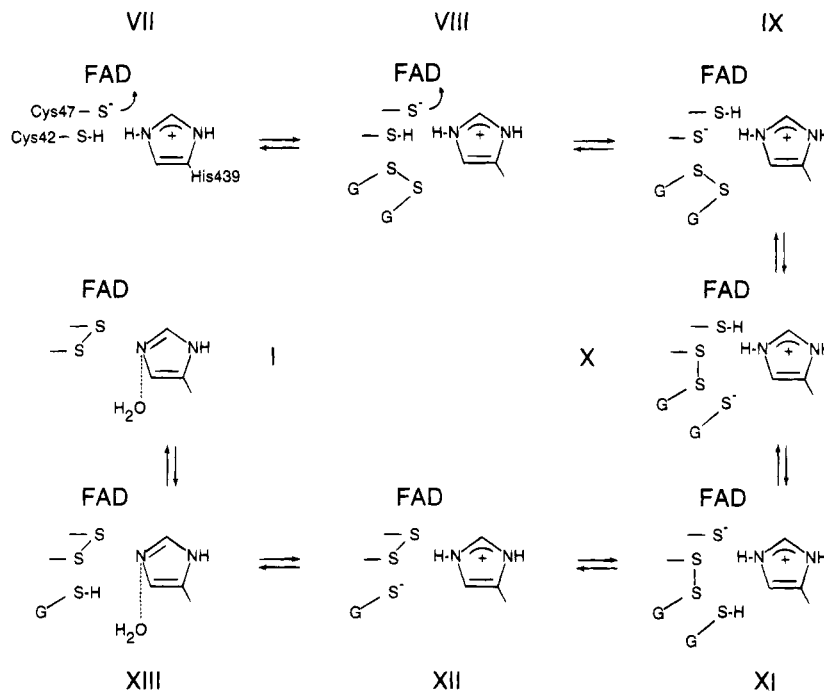
State IV: The covalent intermediate where the protein is covalently bound to the FADH⁻ radical cation.

Step 4 (IV to V): An equilibrium reaction with a rate constant of 110 s⁻¹. The disulfide bond is cleaved, regenerating the free thiols (V).

State V: The state where the protein is re-reduced by NADPH, regenerating the free thiols (Cys42-S-H and Cys47-S-H).

Step 5 (V to VI): An equilibrium reaction with a rate constant of 110 s⁻¹. The protein is re-reduced by NADPH, regenerating the free thiols (Cys42-S-H and Cys47-S-H).

State VI: The state where the protein is re-reduced by NADPH, regenerating the free thiols (Cys42-S-H and Cys47-S-H).

Scheme 2: Intermediates in the Oxidative Half-Reaction^a

glutathione on the mixed disulfide (species X to species IX) (Wong et al., 1988). The mechanism proposed for glutathione reductase in schemes 1 and 2 is based on an earlier version which suggested an additional role for the active site acid/base catalyst in the transfer of electrons from FADH^- to the disulfide by stabilization of the nascent thiolate anion of Cys⁴⁷ in species VI (Arscott et al., 1981). The rate of electron transfer from FADH^- to disulfide has been shown to be diminished in the closely related enzyme, liponamide dehydrogenase, where the acid-base catalyst has been altered (Williams et al., 1989; Benen et al., 1991). We present here data supporting this additional role in glutathione reductase.

MATERIALS AND METHODS

Site-directed mutagenesis of the *gor* gene from *Escherichia coli* that codes for glutathione reductase was effected, transformed cells were grown, and glutathione reductase was purified as previously described (Deonarain et al., 1989). The C47S/H439A¹ mutant was constructed from the C47S and H439A single mutants by the procedure used to construct the C42A/H439A mutant (Deonarain et al., 1990). Enzyme concentration is expressed as the concentration of enzyme-bound FAD using an extinction coefficient of $11\,300\text{ M}^{-1}\text{ cm}^{-1}$ at 462 or 460 nm for wild-type and H439A, respectively. The extinction coefficient of the mutants was determined by removing the bound FAD using either 5 M guanidine hydrochloride or 2% SDS and comparing the resulting absorbance at 448 nm to that of free FAD and wild-type enzyme under the same conditions. NADPH, GSSG, and the Good buffers were of analytical grade and obtained from Sigma Chemical Co.

Steady State Kinetics. Steady state assays used the Good buffers, thereby avoiding the competitive ligand binding in the pyridine nucleotide-binding site which has been observed for the phosphate ion (Staal & Veeger, 1969). All assays were done in triplicate with SD < $\pm 10\%$ and in a 2 mL final volume, at 25 °C, with 0.3 mM EDTA and 100 mM buffers as follows: pH 5.6 MES; pH 6.2–8.1 HEPES; pH 8.7–9.3 CHES; pH 9.8 CAPS. Initial velocities of oxidation of 100 μM NADPH were measured at 340 nm using an extinction coefficient of $6220\text{ M}^{-1}\text{ cm}^{-1}$. Six concentrations of the variable substrate, GSSG were used. The resulting turnover numbers at each pH, expressed as mol NADPH oxidized per minute per mol of enzyme-bound FAD, versus concentration of the varied substrate were fit to a rectangular hyperbola using a program written in ASYST (L. D. Arscott and C. H. Williams, Jr., unpublished results) to give V_{max} and an apparent K_{m} . These values were then graphically fitted to equations assuming either one or two pK_{a} values, using a fitting routine similar to that described below.

Rapid Reaction Kinetics. The rapid kinetics of both wild-type and H439A glutathione reductase were measured in a stopped-flow spectrophotometer designed by Arscott and Ballou, University of Michigan, and built in the VA laboratory. The optical path is 2 cm. A quartz light pipe directs half the emerging light beam to a Tracor Northern TN-6500 rapid scan spectrometer with diode array detector (350–700 nm) and the other half via a double monochromator (variable wavelength) to a photomultiplier tube detector. The dead time of the instrument is 4 ms, and the scan time of the diode array is 5.4 ms. The photomultiplier tube output is interfaced to a Gateway2000 486/33C computer through a Data Translation DT2801-A high speed data acquisition board. Software for data acquisition was written

in ASYST. The data were analyzed by fitting either to a single or to a sum of multiple exponents (Marquardt, 1963) using a program written in PASCAL in Dr. D. A. Ballou's Laboratory, University of Michigan. The resulting observed rate constants (k_{obs}) were fitted to a rectangular hyperbola to determine the maximum rate constant under conditions of saturating and the apparent K_{d} . All reactions were done anaerobically (Williams et al., 1979). The concentration of glutathione reductase after mixing was 8–15 μM . Both wild-type glutathione reductase and H439A were reduced by tipping 5–8 mL of the enzyme buffered with 0.05 M HEPES, pH 7.6 from the main space of an anaerobic tonometer into the side arm containing sodium borohydride dissolved in 10 μL of 0.2 N NaOH (ca. 50-fold excess over enzyme–FAD). This last step ensures that there is a precise amount of reductant, since over-reduction to the EH_4 form occurs in some of the mutants studied. The rate of hydrolysis of borohydride at pH 7.5 is $0.03\text{--}0.04\text{ s}^{-1}$ (Davis & Swain, 1960), thus the rate of enzyme reduction to EH_2 must be balanced against the rate of borohydride hydrolysis so that EH_2 is fully formed and excess borohydride is hydrolyzed before the reaction with GSSG. All reactions were at 4 °C except the oxidative half-reaction of H439A with GSSG, which was at 25 °C. Both the reduction with NADPH and oxidation with GSSG were initiated by rapidly mixing equal volumes of enzyme with either of these reactants.

RESULTS

Kinetic Parameters as a Function of pH. The catalytic properties of the H439A (Deonarain et al., 1989) and H439Q (Berry et al., 1989) mutants have been published. They showed k_{cat} values of 0.3% and 1%, respectively, compared with wild-type enzyme, at pH 7.6. The change of the acid–base catalyst effected in H439A eliminated the possibility of H-bonding allowed in H439Q. The very low k_{cat} values demonstrate the crucial function played by the histidine residue and suggest that a glutamine residue only minimally replaces this function. It is not possible to accurately determine the K_{m} for NADPH spectrophotometrically since it is less than 2 μM (Berry et al., 1989; Deonarain et al., 1989). We have extended this study by evaluating the effect of pH on the kinetic parameters to describe the function of the histidine more fully by replacing it with a nontitratable residue. Figure 1A shows a bell-shaped profile for k_{catgssg} as a function of pH, with pK_{a} values of 6.3 and 7.6 associated with the enzyme–substrate complex. The pH optimum is 6.9. Figure 1B shows $k_{\text{catgssg}}/K_{\text{mgssg}}$ as a function of pH for H439A, indicating a pK_{a} of 7.4 for the free enzyme (or free glutathione disulfide).

The Reductive Half-Reaction for H439A and Wild-Type Glutathione Reductase. The expected decrease in absorbance at 460 nm was not observed in the step attributed to the reduction of the flavin in the previous study of the reductive half-reaction (Huber & Brandt, 1980). We suggest, based on the experiments reported here, that this was because the rate of flavin reoxidation was of the same order of magnitude as the rate of FAD reduction. Reduction of H439A by NADPH, in contrast with the wild-type enzyme, allows direct observation of flavin reduction. The results are shown in Figure 2 and Scheme 1 depicts the reductive half-reaction. The NADPH–FAD charge transfer complex (species II) is formed in the dead time of the instrument. The spectrum of the NADPH–FAD charge transfer complex is not shown.

¹ Abbreviations: E_{ox} , oxidized enzyme; EH_2 , 2-electron reduced enzyme; EH_4 , 4-electron reduced enzyme; GSH, glutathione; GSSG (or gssg), glutathione disulfide; HEPES, *N*-(2-hydroxyethyl)piperazine-*N'*-(2-ethanesulfonic acid); MES, 2-(*N*-morpholino)ethanesulfonic acid; CHES, 2-(*N*-cyclohexylamino)ethanesulfonic acid; CAPS, 3-(cyclohexylamine)-1-propanesulfonic acid. Site-directed mutation of glutathione reductase: H439A or H439Q, with histidine-439 replaced with an alanine or glutamine residue, respectively; C42A, with cysteine-42 replaced with an alanine residue; C42A/H439A, with cysteine-42 and histidine-439 replaced with alanine residues; C47S, with cysteine-47 replaced with a serine residue; C47S/H439A, with cysteine-47 and histidine-439 replaced with a serine and an alanine residue, respectively.

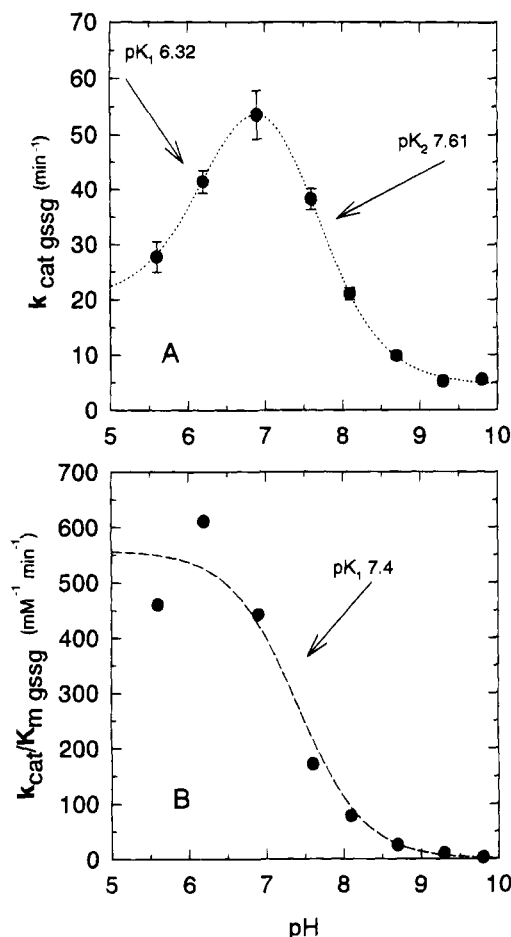


FIGURE 1: Dependence of V_{max} and V_{max}/K_m of H439A on pH. All data points are extrapolated from plots of rate vs [GSSG] as the variable substrate, with NADPH at a saturating concentration of 100 μM . (A) Dotted line represents a best fit theoretical bell-shaped curve with $pK_1 = 6.32 \pm 0.06$ and $pK_2 = 7.61 \pm 0.03$. (B) Dashed line represents the best fit to a single proton ionization with $pK_1 = 7.4 \pm 0.2$.

It can be approximated by back-extrapolation and has slightly diminished absorbance at 460 nm and increased absorbance at 590 nm (Massey et al., 1970). (This species is prominent in the experiment of Figure 4.)

Reduction of FAD in H439A is observed at two wavelengths, as a decrease at 460 nm and as an increase at 670 nm, indicating formation of an FADH^- - NADP^+ charge transfer complex (species III). Spectrum 2 is a scan completed at 9.4 ms (4 ms dead time + 5.4 ms scan time), and spectra 3 and 4 show further progression of FAD reduction. Subsequent passage of electrons from FADH^- to the disulfide, observed as an increase at 460 nm and 525 nm and a decrease at 670 nm, is shown in curves 5 and 6 of Figure 2 (species VI). It is the slow rate of flavin reoxidation and disulfide reduction that allows direct observation of the preceding FAD reduction. It should be noted that between 30 and 120 ms (time lapse between spectra 4 and 5) there is no further flavin reduction (inset of Figure 2). Considerable oxidized flavin remains (curve 4) in this reaction with only 1 equiv of NADPH, as expected. At higher ratios of reductant to enzyme, the 460 nm peak is further diminished.

The kinetics of the reaction are shown in the inset of Figure 2 on a time scale of 1 s. The rate of FAD reduction is dependent on the NADPH concentration and is 250 s^{-1} at infinite NADPH (Table 1). The rate of FADH^- reoxidation

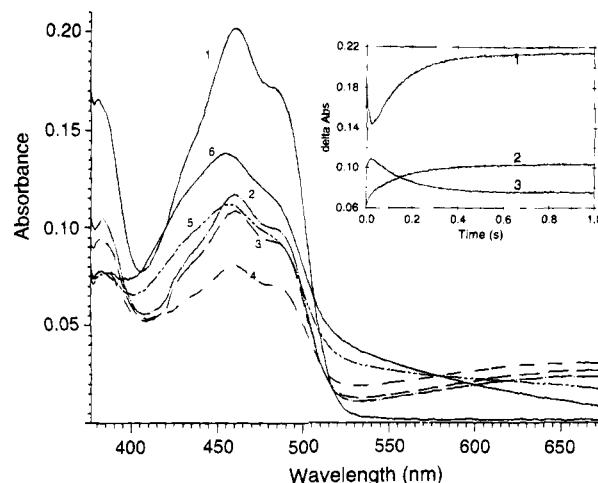


FIGURE 2: Reaction of H439A with NADPH. Anaerobic reduction of 10 μM H439A with 10 μM NADPH (concentrations are after mixing) in 0.05 M HEPES buffer, pH 7.6, 4 $^{\circ}\text{C}$. Times in ms for each curve are as follows: 1, oxidized; 2, 9.4; 3, 14.8; 4, 31.1; 5, 117.4; 6, 275. The order of the spectra from bottom to top at 650 nm is 1, 6, 5, 2, 3, and 4. The signal to noise ratio was good at wavelengths greater than 400 nm, but the data have been smoothed to allow better discrimination between spectra. Inset: kinetic traces with fitted curves. Curves: 1, 460 nm; 2, 525 nm; 3, 670 nm.

is very slow, 6.7 s^{-1} , and is rate-limiting in the overall half-reaction. This rate is independent of the NADPH concentration, as would be expected for an intramolecular electron transfer step. The disparate rates are clearly seen in curves 1 and 3 which show data from 460 nm and 670 nm (Figure 2, inset). The change at 525 nm (curve 2, Figure 2, inset) is small in the fast phase, but the formation of the thiolate-FAD charge transfer complex is clearly seen at this wavelength, and the rate is the same as that of the slow phase observed at the other two wavelengths.

The transfer of electrons from reduced flavin to the disulfide is fast in the reductive half-reaction of wild-type glutathione reductase, in contrast with the slow rate observed with H439A. Thus, in wild-type enzyme, direct observation of FAD reduction is obscured by its reoxidation. The data shown in Figure 3 are from a reaction of 1 equiv of NADPH per enzyme FAD. At no point in the time course is the absorbance at 460 nm low, as would be associated with reduced flavin. In the 440–460 nm region, two phases are discernible after the deadtime spectrum, curve 2: 2 to 3 to 4 where the extinction drops and the peak position shifts very slightly to lower wavelengths and 4 to 5 to 6 where the extinction rises and the peak position shifts approximately 7 nm further to lower wavelengths. At 540 nm, the absorbance rises in a biphasic manner. Both wavelengths then indicate at least two processes following the initial spectrum.

The kinetics at three wavelengths are shown in the inset to Figure 3. Curve 1 at 440 nm indicates the end of a very fast process at 330 s^{-1} , followed by another fast reaction at 270 s^{-1} and finally a slow change at 14 s^{-1} . This pattern is confirmed by the data at 670 nm albeit with a low signal to noise ratio. The rates are 310, 245, and 6.5 s^{-1} . Curve 2, with the highest signal to noise ratio, represents the data at 525 nm, giving rates of 110 and 10 s^{-1} (Table 1). Briefly, the rapid reactions are FAD reduction, displacement of NADP^+ by NADPH, and flavin reoxidation. We would argue that FAD reduction is largely cancelled in this time

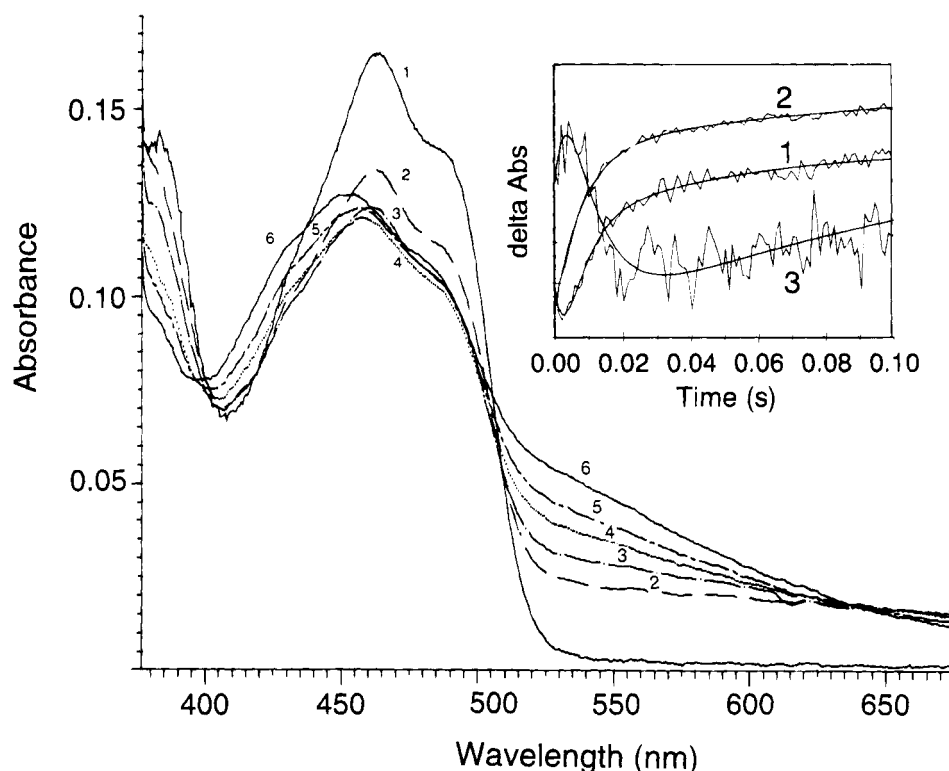


FIGURE 3: Reaction of wild-type glutathione reductase with NADPH. Anaerobic reduction of $7.3 \mu\text{M}$ enzyme with $9.4 \mu\text{M}$ NADPH (after mixing) in 0.05 M HEPES buffer, pH 7.6, 4°C . Times in ms for each curve are as follows: 1, oxidized; 2, 9.4; 3, 14.8; 4, 20.2; 5, 25.7; 6, 117.8. The signal to noise ratio was good at wavelengths greater than 400 nm , but the data have been smoothed to allow better discrimination between spectra. Inset: kinetic traces with fitted curves. Wavelength and full scale absorbance difference are, respectively, as follows: curve 1, 440 nm , 0.027 ; curve 2, 525 nm , 0.042 ; curve 3, 670 nm , 0.007 .

Table 1: Rate Constants for the Reductive Half-Reaction^a

	$k_1 \text{ (s}^{-1}\text{)}$	$k_2 \text{ (s}^{-1}\text{)}$	$k_3 \text{ (s}^{-1}\text{)}$
H439A			
460 nm	250	6.8	
525 nm		6.1	
670 nm	220	7.3	
wild type			
440 nm	330	270	14
525 nm		110	10
670 nm	310	245	6.5

^a Formation of the NADPH–FAD charge transfer complex is fast—complete in the deadtime of the instrument.

frame in the $420\text{--}460 \text{ nm}$ region by the subsequent fast processes. The rate of FAD reduction is dependent on the NADPH concentration, and the rates in Table 1 are limiting values. The rates of 270 and 245 s^{-1} measured at 440 and 670 nm , respectively, are associated primarily with displacement of NADP^+ by NADPH, while that of 110 s^{-1} determined at 525 nm is associated with flavin reoxidation and formation of thiolate–FAD charge transfer.

The reductive half-reaction was investigated for several other altered forms of glutathione reductase, C42A, C42A/H439A, C47S, and C47S/H439A, none of which has a redox active disulfide. It was thought that this would allow measurement of the rate of flavin reduction, as subsequent electron transfer to the disulfide cannot occur. In all cases there was rapid reduction of the FAD, but the extent of reduction was only approximately 10% (cf. Vanoni et al., 1990). Figure 4 shows the reaction of 50 equiv of NADPH with C47S at pH 6.1. Because of the limited extent of the reaction, the rates could only be estimated: C42A, $250 \pm 20 \text{ s}^{-1}$; C42A/H439A, $280 \pm 40 \text{ s}^{-1}$; C47S, $375 \pm 80 \text{ s}^{-1}$;

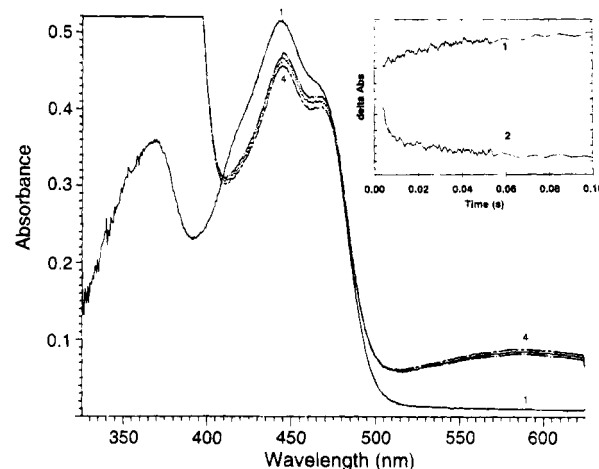


FIGURE 4: Reduction of C47S by NADPH. Anaerobic reduction of $23.4 \mu\text{M}$ C47S with approximately 50 equiv of NADPH (concentrations are after mixing) in 0.05 M HEPES buffer, pH 6.1, 4°C . Times in ms for each curve are as follows: 1, oxidized; 2, 9.4; 3, 14.8; 4, 58.2. Inset: kinetic traces are offset 4 ms to reflect the dead time, fitted curves extrapolate to zero time. Wavelength and full scale absorbance difference are, respectively, as follows: curve 1, 610 nm , 0.030 ; curve 2, 446 nm , 0.070 .

C47S/H439A, $280 \pm 30 \text{ s}^{-1}$. Thus, the rate of flavin reduction is approximately 300 s^{-1} in wild-type enzyme and in all of the mutants. At equilibrium, the absorbance at 590 nm due to the NADPH–FAD charge transfer complex is prominent (species II).

Thus, the redox potential of the FAD in forms of glutathione reductase lacking the disulfide is very low, -449 mV at pH 8.4 for C47S, as estimated by equilibration with methyl viologen using the xanthine/xanthine oxidase system

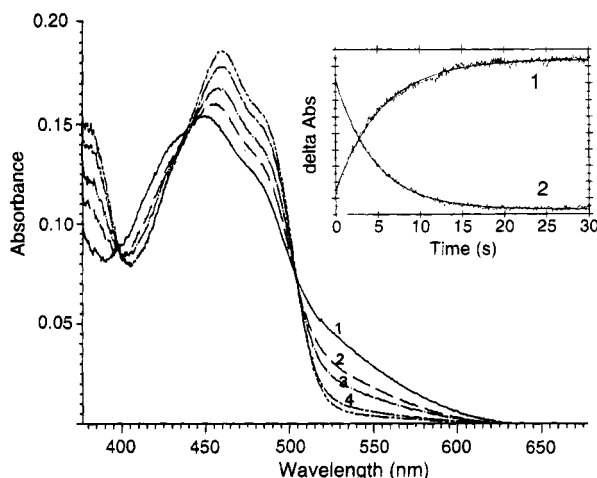


FIGURE 5: Oxidation of borohydride-reduced H439A with glutathione disulfide. Anaerobic reaction of 8.8 μM reduced enzyme with 50.0 μM GSSG (after mixing) in 0.05 M HEPES buffer, pH 7.6, 25 $^{\circ}\text{C}$. Time in s for each curve are as follows: 1, reduced enzyme; 2, 2.0; 3, 4.6; 4, 10.1; 5, 21.2. Inset: kinetic traces with fitted curves. Wavelength and full scale absorbance difference are, respectively, as follows: 1, 460 nm, 0.050; 2, 525 nm, 0.060.

as the electron source (Massey, 1990). This would indicate a potential of -366 mV at pH 7.0 or approximately 38 mV more negative than the potential of NADPH at pH 7.0 (Engel & Dalziel, 1967). The low pH should give a greater extent of reaction since the relative redox potentials of the $\text{NADP}^+/\text{NADPH}$ and FAD/FADH_2 couples become more favorable for FAD reduction at low pH (Matthews & Williams, 1976). However, the observed equilibrium at pH 6.1 is even less favorable than would be predicted on the basis of the redox potential, suggesting an influence on the potential due to differential binding of pyridine nucleotide to the oxidized and reduced enzyme forms.

Oxidative Half-Reaction of H439A and Wild-Type Glutathione Reductase. The oxidative half-reaction mixing borohydride-reduced H439A and glutathione disulfide is monophasic and at 25 $^{\circ}\text{C}$ is very slow with a limiting rate of 0.82 s^{-1} under conditions of saturating glutathione disulfide (Figure 5). This contrasts with the wild-type enzyme, where the same reaction measured at 4 $^{\circ}\text{C}$ has a limiting rate of 490 s^{-1} or at least 600-fold faster than the H439A mutant enzyme, without considering the 21 $^{\circ}\text{C}$ difference in temperature (Figure 6). The turnover number for the yeast enzyme has been determined at 5 and at 25 $^{\circ}\text{C}$, and the difference is 7.6-fold (Williams, 1992). This provides a reasonable temperature correction to be applied to the rate of reoxidation of wild type enzyme suggesting a rate at 25 $^{\circ}\text{C}$ of 3900 s^{-1} . Clearly, the acid-base catalyst is crucial in this half-reaction. As proposed previously, it is likely that it serves to protonate the thiolate anion of the first departing molecule of glutathione, thereby inhibiting the back-reaction—attack of glutathione thiolate on the mixed disulfide between the other glutathione and Cys^{42} (species X and IX, Scheme 2) (Wong et al., 1988).

DISCUSSION

The acid-base catalyst in glutathione reductase and lipoamide dehydrogenase is a histidine residue (Figure 7). Altered forms of these enzymes have been prepared by site-directed mutagenesis of this residue (Deonarain et al., 1989, 1990; Williams et al., 1989; Benen et al., 1991). In all cases

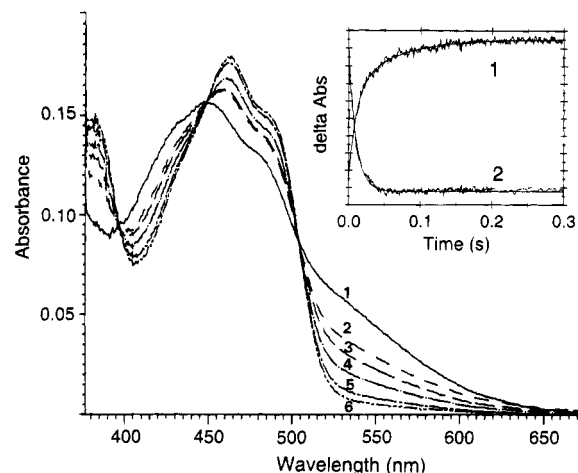


FIGURE 6: Oxidation of borohydride reduced wild-type glutathione reductase with glutathione disulfide. Anaerobic reaction of 8.5 μM reduced enzyme with 20.0 μM GSSG (after mixing) in 0.05 M HEPES buffer, pH 7.6, 4 $^{\circ}\text{C}$. Time in ms for each curve are as follows: 1, reduced enzyme; 2, 9.4; 3, 14.8; 4, 20.2; 5, 36.5; 6, 74.4. Inset: kinetic traces with fitted curves. Wavelength and full scale absorbance difference are, respectively, as follows: 1, 462 nm, 0.035; 2, 525 nm, 0.035.

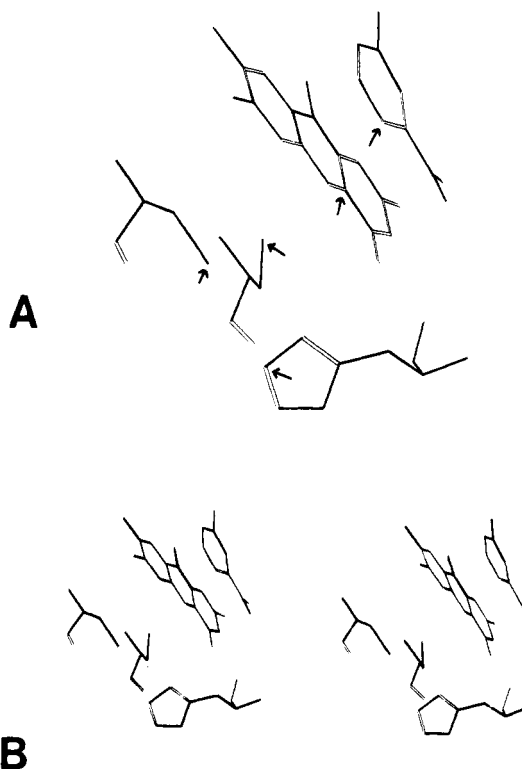


FIGURE 7: Representation of the active site of glutathione reductase. The view is from the *si* side and the pyrimidine ring end of the isoalloxazine ring, with His⁴⁶⁷, Cys⁵⁸, and Cys⁶³ in the foreground and the pyridinium ring in the background. A. The following atoms have been marked: sulfurs of Cys⁵⁸ and Cys⁶³, N3 of His⁴⁶⁷, C4a of the isoalloxazine ring, and C4' of the pyridinium ring. B. Stereo. The representations are from Sybyl software, Tripos Associates, Inc., using the human erythrocyte glutathione reductase structure (Karplus & Schulz, 1987).

the activity is diminished in excess of 100 fold. In lipoamide dehydrogenase, the acid-base catalyst serves to deprotonate dihydrolipoamide, creating a nucleophilic thiolate for attack on the enzyme disulfide, and stabilizes the resulting enzyme thiolate (Matthews & Williams, 1976). The acid catalyst in glutathione reductase stabilizes the enzyme thiolate as it

attacks glutathione disulfide and protonates the first departing glutathione molecule (Wong et al., 1988; Deonarain et al., 1990). Thus, the catalyst in both enzymes functions in the first half of the dithiol–disulfide interchange. But, in stabilizing the enzyme thiolate, the imidazolium potentially functions in FAD reduction in lipoamide dehydrogenase or in flavin reoxidation in glutathione reductase (Arscott et al., 1981). Such a subsidiary role has been demonstrated in lipoamide dehydrogenase (Williams et al., 1989; Benen et al., 1991), and the present study seeks to extend the analogy to glutathione reductase.

The pH dependence of k_{catgssg} gives a pH optimum of 6.9 for the remaining activity of H439A. Activity is dependent on deprotonation of a residue with an apparent pK_a of 6.3 and on protonation of a residue with an apparent pK_a of 7.6 (Figure 1A). The pK_a values are associated with groups on the EH_2 –GSSG complex. The pH dependence of $k_{\text{catgssg}}/K_{\text{mgssg}}$ reveals a protonated group on EH_2 (or free glutathione disulfide) required for activity and having an apparent pK_a value of approximately 7.4 (Figure 1B).

The most notable feature of the data from H439A is that any pK_a at 9.2 attributable to the acid–base catalyst is missing, as expected (Figure 1). The pK_a of 7.4–7.6 is probably the unidentified group observed in the yeast and erythrocyte enzymes with pK_a values of 7.8–8.4. Alternatively, it could reflect the ionization of the γ -glutamyl moiety of glutathione disulfide. Finally, the pK_a of 6.3 is attributed to one of the thiols.² The pK_a is nominally higher than in the yeast enzyme (6.2) because His⁴³⁹, a factor contributing to the low pK_a values of the thiols, has been replaced. However, two other factors that remain are important in stabilizing the thiols as thiolates (Karplus & Schulz, 1989): the dipole created by the α -helix beginning with the loop containing the thiols (the positive end, amino-terminus) and hydrogen bonding to Thr³⁸⁹ (erythrocyte numbering).

Removal of the active site acid–base catalyst by replacing His⁴³⁹ with an alanine residue has its major effect on the oxidative half-reaction, as would be expected (cf. Figures 5 and 6). The rate of reoxidation of borohydride-reduced H439A is slowed by at least 600-fold relative to the same reaction in wild-type glutathione reductase. It should be mentioned that the residual activity in H439A is not unexpected, since a needed proton can always be supplied by the solvent, albeit inefficiently (Deonarian et al., 1989).

Intermediates in the oxidative half-reaction are depicted in Scheme 2 in which the numbering is consecutive with Scheme 1. Species VII is an EH_2 form rather than the EH^- form used in a similar representation of this half-reaction (Wong et al., 1988) because the pK_a for the deprotonation of EH_2 appears to be higher than the pH optimum for catalysis. The pK_a associated with the transition between EH^- and EH_2 can, in principle, be detected by measuring the pH dependence of the enzyme redox potential (E/EH_2). The pK_a for this transition is 7.4 for glutathione reductase from yeast (Arscott et al., 1991). With the enzyme from *E. coli*, the change in slope is less clear, but the pK_a is higher than with the yeast enzyme, perhaps as high as 8.6 (Veine et al., 1994). Therefore, with the *E. coli* enzyme, EH_2 is the major reactive species, given the pH optimum of approximately 7 for both enzymes. Species VII is the major

EH_2 species at equilibrium, with the protons depicted on the acid–base catalyst and the interchange thiol, Cys⁴², the two groups having the highest pK_a values. After glutathione disulfide binding (species VIII), and before nucleophilic attack, the interchange thiol must be deprotonated (species IX). Formation of the mixed disulfide follows (species X). The data of Wong et al. (1988) suggest that the back-reaction (species X to IX) is facile. The major function of the acid catalyst then is to protonate the departing glutathione, after which the acid–base catalyst is reprotonated by the Cys⁴⁷ thiol (species X to XI). The reaction species XI to species XII includes the first step in the second thiol–disulfide interchange, breakdown of the mixed disulfide, and reformation of the enzyme disulfide. The thiolate of the second glutathione is protonated (species XII to XIII) and glutathione dissociates (species XIII to I). In H439A, with the imidazolium proton no longer available, the rate of the back reaction is significant (species X to species IX); that is, the nascent ionized glutathione can attack the mixed disulfide formed between the other glutathione and the interchange thiol of the enzyme, Cys⁴² (Wong et al., 1988).

Turning to the reductive half-reaction, the rate of intramolecular electron transfer from FADH^- to the active site disulfide in H439A is reduced 16-fold compared with wild-type enzyme. This indicates that the acid–base catalyst plays a role in the disulfide reduction step consistent with the mechanism proposed previously (Arscott et al., 1981). A similar observation has been made with the closely related enzyme, lipoamide dehydrogenase (Williams et al., 1989; Benen et al., 1991). This slowing of the rate of reoxidation of reduced flavin allows direct observation of the preceding step, FAD reduction in H439A (Figure 2 and Scheme 1). This reaction is largely obscured in wild-type enzyme since it is followed by rapid flavin reoxidation. Concurrent displacement of NADP^+ by NADPH further obscures flavin reoxidation in wild type enzyme (Bulger and Brandt, 1971). The product of FAD reduction is the FADH^- – NADP^+ charge transfer complex (species III), and its formation can be clearly observed in H439A at 670 nm. The slow reoxidation of reduced flavin at only 6.7 s^{-1} is easily measured at 460 and 670 nm. The thiolate–FAD charge transfer complex forms as the disulfide is reduced and a proton is transferred from the flavin-interacting thiol, Cys⁴⁷, to the interchange thiol, Cys⁴². Figure 7 shows that the pyridinium and isoalloxazine rings are stacked and thus can form a unified acceptor for the thiolate donor. NADPH enhances the thiolate–FAD charge transfer extinction at 540 nm (species VI), while NADP^+ causes a shift to 580 nm (Williams et al., 1976).

The insights gained in the study of the H439A reductive half-reaction allow a more complete interpretation of the same reaction in wild-type enzyme. Since the absorbance at 460 nm would decrease on reduction of FAD and increase on reoxidation of flavin, and since they are happening at sequential rates in excess of 100 s^{-1} , there will be very little net change in the 440–460 nm region (Figure 3). The changes can be seen in two spectral phases, curves 2 to 3 to 4 (down) and curves 4 to 5 to 6 (up and shift to shorter wavelengths). That there has been extensive flavin reoxidation in the first 20 ms is obvious from the kinetics observed at 525 nm. The increase in absorbance at 525 nm reflects primarily the formation of the thiolate–FAD charge transfer complex (species VI, Scheme 1). With a rate constant of

² K. K. Wong and J. S. Blanchard, Albert Einstein College of Medicine, personal communication.

110 s^{-1} , more than 7/8 of the extinction change is complete within 20 ms. This is not obscured either by the formation of the NADPH–FAD charge transfer complex (species II) which is complete in the dead time or by the FADH[−]–NADP⁺ charge transfer complex (species III) which absorbs minimally at 525 nm (Massey & Palmer, 1962). In an effort to observe FAD reduction without the subsequent flavin reoxidation, mutants lacking the disulfide (e.g., C47S) were utilized, albeit with a very unfavorable equilibrium (Figure 4). The rate of reduction is approximately 300 s^{-1} , as is the case with wild-type glutathione reductase. C47S and other forms lacking the disulfide offer an opportunity to observe the NADPH–FAD charge transfer complex absorbing maximally at 590 nm since the equilibrium between it and the FADH[−]–NADP⁺ charge transfer complex favors the former (species II and III).

The experiments reported in this paper illustrate the utility of using altered forms of an enzyme to study reactions in the catalytic path that are inaccessible in the wild-type enzyme. Not only does this reveal the steps in which the altered residue is involved, but it can allow measurement of steps which are otherwise too fast for the rates to be determined. H439A, with the acid–base catalyst removed, is severely limited in certain steps of catalysis. This confirmed the obvious involvement of the acid–base catalyst in the oxidative half-reaction, but also demonstrated its involvement in the transfer of the reducing equivalent from reduced flavin to the redox active disulfide. The rapid rate of this step obscured the measurement of the rate of FAD reduction in wild-type enzyme but the rate of this step was easily determined in H439A.

ACKNOWLEDGMENT

The authors are grateful to Dr. John Blanchard for communicating the yeast glutathione reductase data and for many helpful discussions, to Ms. Cathy Luschinsky Drennan for suggesting the experiments with altered forms lacking the redox active disulfide, and to Ms. Donna Veine for preparing the enzyme and for help with the manuscript.

REFERENCES

- Arscott, L. D., Thorpe, C., & Williams, C. H., Jr. (1981) *Biochemistry* 20, 1513–1528.
- Arscott, L. D., Veine, D. M., & Williams, C. H., Jr. (1991) in *Flavins and Flavoproteins* (Curti, B., Zanetti, G., & Ronchi, S., Eds.) pp 529–532, Walter de Gruyter and Co., Berlin.
- Benen, J., Van Berkel, W., Zak, Z., Visser, T., Veeger, C., & de Kok, A. (1991) *Eur. J. Biochem.* 202, 863–872.
- Berry, A., Scrutton, N. S., & Perham, R. N. (1989) *Biochemistry* 28, 1264–1269.
- Bulger, J. E., & Brandt, K. G. (1971) *J. Biol. Chem.* 240, 5578–5587.
- Davis, R. E., & Swain, C. G. (1960) *J. Am. Chem. Soc.* 82, 5949–5950.
- Deonarain, M. P., Berry, A., Scrutton, N. S., & Perham, R. N. (1989) *Biochemistry* 28, 9602–9607.
- Deonarain, M. P., Scrutton, N. S., Berry, A., & Perham, R. N. (1990) *Proc. Roy. Soc. Lond. B* 241, 179–186.
- Engel, P. C., & Dalziel, K. (1967) *Biochem. J.* 105, 691–695.
- Huber, P. W., & Brandt, K. G. (1980) *Biochemistry* 19, 4568–4575.
- Karplus, P. A., & Schulz, G. E. (1987) *J. Mol. Biol.* 95, 701–729.
- Karplus, P. A., & Schulz, G. E. (1989) *J. Mol. Biol.* 210, 163–180.
- Marquardt, D. W. (1963) *J. Soc. Ind. Appl. Math.* 11, 431–441.
- Massey, V. (1990) in *Flavins and Flavoproteins* (Curti, B., Zanetti, G., & Ronchi, S., Eds.) pp 59–66, Walter de Gruyter and Co., Berlin.
- Massey, V., & Palmer, G. (1962) *J. Biol. Chem.* 237, 2347–2358.
- Massey, V., Matthews, R. G., Foust, G. P., Howell, L. G., Williams, C. H., Jr., Zanetti, G., & Ronchi, S. (1970) in *Pyridine Nucleotide-Dependent Dehydrogenases* (Sund, H., Ed.) pp 393–409, Springer-Verlag, Berlin.
- Matthews, R. G., & Williams, C. H., Jr. (1976) *J. Biol. Chem.* 251, 3956–3964.
- Staal, G. E. J., & Veeger, C. (1969) *Biochim. Biophys. Acta* 185, 49–62.
- Vanoni, M. A., Wong, K. K., Ballou, D. P., & Blanchard, J. S. (1990) *Biochemistry* 29, 5790–5796.
- Veine, D. M., Arscott, L. D., & Williams, C. H., Jr. (1994) in *Flavins and Flavoproteins* (Yagi, K., Ed.) pp 496–500, Walter de Gruyter and Co., Berlin.
- Williams, C. H., Jr. (1992) in *Chemistry and Biochemistry of Flavoenzymes* (Müller, F., Ed.) Vol. III, pp 121–211, CRC Press, Boca Raton.
- Williams, C. H., Jr., Arscott, L. D., & Jones, E. T. (1976) in *Flavin and Flavoproteins, Fifth International Symposium* (Singer, T. P., Ed.) pp 455–463, Elsevier Scientific Publishing Co., New York.
- Williams, C. H., Jr., Arscott, L. D., Matthews, R. G., Thorpe, C., & Wilkinson, K. D. (1979) in *Methods in Enzymology—Vitamins and Coenzymes* (McCormick, D. B., & Wright, L. D., Eds.) pp 185–198, Academic Press, New York.
- Williams, C. H., Jr., Allison, N., Russell, G. C., Prongay, A. J., Arscott, L. D., Datta, S., Sahlman, L., & Guest, J. R. (1989) *Ann. NY Acad. Sci.* 573, 55–65.
- Wong, K. K., Vanoni, M. A., & Blanchard, J. S. (1988) *Biochemistry* 27, 7091–7096.